Broken discrete and continuous symmetries in two-dimensional spiral antiferromagnets

2013 J. Phys.: Condens. Matter 25 465602

(http://iopscience.iop.org/0953-8984/25/46/465602)

IOP PUBLISHING JOURNAL OF PHYSICS: CONDENSED MATTER

J. Phys.: Condens. Matter **25** (2013) 465602 (9pp) doi:10.1088/0953-8984/25/46/465602

Broken discrete and continuous symmetries in two-dimensional spiral antiferromagnets

A Mezio, C N Sposetti, L O Manuel and A E Trumper

Instituto de Física Rosario (CONICET) and Universidad Nacional de Rosario, Boulevard 27 de Febrero 210 bis, (2000) Rosario, Argentina

E-mail: trumper@ifir-conicet.gov.ar

Received 22 August 2013, in final form 19 September 2013
Published 23 October 2013
Online at stacks.iop.org/JPhysCM/25/465602

Abstract

We study the occurrence of symmetry breaking, at zero and finite temperatures, in the J_1–J_3 antiferromagnetic Heisenberg model on the square lattice using Schwinger boson mean field theory. For spin-$\frac{1}{2}$ the ground state always breaks the SU(2) symmetry with a continuous quasi-critical transition at $J_3/J_1 \sim 0.38$, from Néel to spiral long range order, although local spin fluctuation considerations suggest an intermediate disordered regime around $0.35 \lesssim J_3/J_1 \lesssim 0.5$, in qualitative agreement with recent numerical results. At low temperatures we find a Z_2 broken symmetry region with short range spiral order characterized by an Ising-like nematic order parameter that compares qualitatively well with classical Monte Carlo results. At intermediate temperatures the phase diagram shows regions with collinear short range orders: for $J_3/J_1 < 1$ Néel (π, π) correlations and for $J_3/J_1 > 1$ a novel phase consisting of four decoupled third neighbour sublattices with Néel (π, π) correlations in each one. We conclude that the effect of quantum and thermal fluctuations is to favour collinear correlations even in the strongly frustrated regime.

(Some figures may appear in colour only in the online journal)

1. Introduction

The study of unconventional phases represents a central topic in strongly correlated electron systems. In frustrated quantum antiferromagnets (AFs) the interest is mainly focused on the possible stabilization of two-dimensional (2D) quantum spin liquids [1–3] that preserve all the microscopic symmetries of the Hamiltonian. In fact, in recent years, there has been great interest in the classification of different types of quantum spin liquids based on the projective symmetry group [4–6]. However, the concrete detection of such spin liquids in realistic quantum spin models seems to be still a delicate issue [3, 7–10]. The source of this classification is the mean field wavefunctions based on the bosonic and fermionic representations for the spin operator, originally used in the context of large N theories [11, 12]. The bosonic representation (Schwinger bosons) has the advantage of describing magnetically ordered states [13–15]—which are known in several cases—while quantum spin liquid states can be described by both bosonic and fermionic representations [9, 10, 15].

Another route in the search for unconventional phases due to magnetic frustration has been the study of finite temperature transitions involving the rupture of non-trivial discrete degrees of freedom. This kind of transition has been extensively investigated in the context of the frustrated J_1–J_2 Heisenberg model [2, 16, 17]. Here, the magnetic phase breaks the discrete lattice rotation symmetry from Z_4 to Z_2 with an associated Ising variable that gives a measure of the $(0, \pi)$ and $(\pi, 0)$ magnetic correlations [18], while rotational symmetry is unbroken, as dictated by the Mermin–Wagner theorem [19]. Several analytical [18, 20] and numerical [21] studies on the J_1–J_2 model have confirmed the occurrence of a finite temperature transition to a Z_2 broken symmetry phase that belongs to the Ising universality class. Less explored, however, has been the occurrence of such a transition in the

J_1–J_3 model where, in contrast to the original case, the spin correlations are of spiral type [15, 22, 23]. Classically, for $J_3/J_1 > 1/4$, there are two degenerate incommensurate spiral ground states, $\mathbf{Q} = (Q, Q)$ and $(Q, -Q)$, that are connected by a global rotation followed by a reflexion about y. Then, the global symmetry of the classical ground state is $O(3) \times Z_2$. Classical Monte Carlo calculations [24] predict that a Z_2 broken symmetry phase described by an Ising nematic order parameter (see below) survives within the finite temperatures range (see the inset of figure 6), the transition also being of the Ising universality class. On the other hand, at zero temperature, numerical studies for $S = \frac{1}{2}$ predict the existence of an intermediate disordered regime in the range $0.4 \lesssim J_3/J_1 \lesssim 0.8$ with, probably, short range order (SRO) plaquette and spiral regimes between long range order (LRO) Néel and spiral phases [25–27], while for the special case $J_3/J_1 \simeq 0.5$ there is evidence of a homogeneous spin liquid state [28].

In order to complement the classical Monte Carlo results and to make contact with the zero temperature quantum regime, it is important to investigate the interplay between quantum and thermal fluctuations at low temperatures within a reliable theory. In this sense, it has been shown that the Schwinger boson mean field (SBMF) approach based on the two singlet bond operator scheme [20, 29–31] works very well for several frustrated models. In particular, for a triangular AF, we have recently shown that the zero temperature energy spectrum [32] and the low temperature thermodynamic properties [33] predicted by numerical methods are correctly reproduced. In addition, this mean field scheme provides a qualitatively good description of the finite temperature Ising transition in the J_1–J_2 model [20].

Motivated by these results, in this paper we investigate the occurrence of both the zero temperature SU(2) broken symmetry ground state and the finite temperature Z_2 broken symmetry transition in the frustrated J_1–J_3 Heisenberg model, using the Schwinger boson mean field theory. For the zero temperature quantum phase diagram (figure 2) we show that the two singlet scheme of the SBMF takes correctly into account the effect of frustration J_3/J_1 within the collinear phases leading to qualitative and quantitative differences with respect to previous calculations based on a one singlet scheme [15]. Although for $S = \frac{1}{2}$ the SU(2) symmetry is always broken with a continuous quasi-critical transition at $J_3/J_1 \sim 0.38$, from Néel to spiral long range order (figure 3), local spin fluctuation considerations allow us to estimate a disordered regime $0.35 \lesssim J_3/J_1 \lesssim 0.5$ between the Néel and spiral states in qualitative agreement with recent numerical results [27]. As soon as the temperature increases the finite temperature phase diagram (figure 6) shows a Z_2 broken symmetry phase characterized by finite Ising nematic order with the rotational invariance restored. The behaviour of the critical temperature T_c with frustration, signalled by the vanishing of the nematic order parameter, compares quite well with classical Monte Carlo predictions [24]. As the temperature is further increased two different temperature effects—before reaching the paramagnetic phase—are observed: for $J_3/J_1 < 1$ short range Néel (π, π) correlations are favoured while for $J_3/J_1 > 1$ there is an intermediate novel phase—we have named it $(\pi, \pi)_4$—characterized by four decoupled third neighbour sublattices with AF short range correlations in each one.

2. The Schwinger boson approach within the two singlet scheme

The AF Heisenberg model on a square lattice with first J_1 and third J_3 neighbour interaction is defined as

$$\hat{H} = J_1 \sum_{\langle ij \rangle} \hat{\mathbf{S}}_i \cdot \hat{\mathbf{S}}_j + J_3 \sum_{\langle ik \rangle} \hat{\mathbf{S}}_i \cdot \hat{\mathbf{S}}_k, \tag{1}$$

where $\langle ij \rangle$ and $\langle ik \rangle$ denote first and third neighbours, respectively, on the square lattice. In using the Schwinger boson representation for the spin operators [12],

$$\hat{\mathbf{S}}_i = \tfrac{1}{2} \mathbf{b}_i^\dagger \vec{\sigma} \mathbf{b}_i, \tag{2}$$

with $\mathbf{b}_i^\dagger = (b_{i\uparrow}^\dagger; b_{i\downarrow}^\dagger)$ a spinor composed of the bosonic spin-$\frac{1}{2}$ operators $b_{i\uparrow}^\dagger$ and $b_{i\downarrow}^\dagger$ and $\vec{\sigma} = (\sigma^x, \sigma^y, \sigma^z)$ the Pauli matrices, the condition of $2S$ bosons per site

$$b_{i\uparrow}^\dagger b_{i\uparrow} + b_{i\downarrow}^\dagger b_{i\downarrow} = 2S \tag{3}$$

must be satisfied in order to guarantee a physical Hilbert space. After replacing (2) in the spin–spin interaction terms of (1) they can be written in the following two singlet bond operator scheme:

$$\hat{\mathbf{S}}_i \cdot \hat{\mathbf{S}}_j =: \hat{B}_{ij}^\dagger \hat{B}_{ij} : -\hat{A}_{ij}^\dagger \hat{A}_{ij}, \tag{4}$$

with i and j representing either first or third neighbour sites, and the singlet bond operators $\hat{A}_{ij}$ and $\hat{B}_{ij}$ are defined as

$$\hat{A}_{ij}^\dagger = \tfrac{1}{2} \sum_\sigma \sigma b_{i\sigma}^\dagger b_{j\bar{\sigma}}^\dagger, \qquad \hat{B}_{ij}^\dagger = \tfrac{1}{2} \sum_\sigma b_{i\sigma}^\dagger b_{j\sigma}. \tag{5}$$

We call them singlets because they are rotationally invariant under SU(2) transformations of the spinor $\mathbf{b}_i^\dagger = (b_{i\uparrow}^\dagger; b_{i\downarrow}^\dagger)$. The biquadratic terms of (4) are related to the spin operators as

$$\begin{aligned} \hat{A}_{ij}^\dagger \hat{A}_{ij} &= \frac{1}{4}(\hat{\mathbf{S}}_i - \hat{\mathbf{S}}_j)^2 - \frac{S}{2} \\ : \hat{B}_{ij}^\dagger \hat{B}_{ij} :&= \frac{1}{4}(\hat{\mathbf{S}}_i + \hat{\mathbf{S}}_j)^2 - \frac{S}{2}. \end{aligned} \tag{6}$$

Then, after a mean field decoupling of the above expressions, the mean values of the operators $\hat{A}_{ij}^\dagger$ and $\hat{B}_{ij}^\dagger$ can be immediately associated to antiferromagnetic and ferromagnetic correlations between sites i and j, respectively. Using the identity $: \hat{B}_{ij}^\dagger \hat{B}_{ij} : + \hat{A}_{ij}^\dagger \hat{A}_{ij} = S^2$ it is possible to write down the spin interaction (4) in terms of either singlet operator, $\hat{B}_{ij}$ or $\hat{A}_{ij}$, and study independently pure ferromagnetic or antiferromagnetic phases, respectively [11]. For frustrated systems, where quantum disordered phases are expected, there are two schemes of calculation: one takes advantage of the above identity and uses only $\hat{A}_{ij}$ operators [15] while the other one keeps both the $\hat{B}_{ij}$ and $\hat{A}_{ij}$ operators [29]. In principle, both schemes are equivalent, but at the mean field

level the two singlet bond scheme has been shown to be significantly more accurate in describing the magnetically ordered regions of several frustrated models [29, 30, 32, 33]. More recently, this scheme has been used to explore the possible existence of completely symmetric [5, 9] and weakly symmetric—chiral—spin liquid states [6] within the context of the projective symmetry group. Therefore, the two singlet scheme seems to be a more proper and versatile framework to investigate ordered and spin liquid phases in a unified way.

2.1. The mean field decoupling

Performing the standard procedure [29], the spin–spin interaction (4) is replaced in the Hamiltonian (1) along with the introduction of a Lagrange multiplier λ so as to fulfil on average the constraint (3). After a mean field decoupling, with $A_{ij} = \langle \hat{A}_{ij} \rangle = \langle \hat{A}_{ij}^{\dagger} \rangle$ and $B_{ij} = \langle \hat{B}_{ij} \rangle = \langle \hat{B}_{ij}^{\dagger} \rangle$, and Fourier transforming the Schwinger bosons to k-space the quadratic mean field Hamiltonian results,

$$\begin{aligned} \hat{H}_{\mathrm{MF}} = \sum_{\mathbf{k}} [& (\gamma_{\mathbf{k}}^{B} + \lambda)(b_{\mathbf{k}\uparrow}^{\dagger} b_{\mathbf{k}\uparrow} + b_{-\mathbf{k}\downarrow}^{\dagger} b_{-\mathbf{k}\downarrow}) \\ & + \mathrm{i}\, \gamma_{\mathbf{k}}^{A} b_{\mathbf{k}\uparrow}^{\dagger} b_{-\mathbf{k}\downarrow}^{\dagger} - \mathrm{i} \gamma_{\mathbf{k}}^{A} b_{\mathbf{k}\uparrow} b_{-\mathbf{k}\downarrow}] \\ & - E_{\mathrm{MF}} - 2S\lambda N_{\mathrm{s}}, \end{aligned} \tag{7}$$

where

$$E_{\mathrm{MF}} = \frac{N_{\mathrm{s}}}{2} \sum_{\delta} J_{\delta} [B_{\delta}^{2} - A_{\delta}^{2}]$$

and

$$\gamma_{\mathbf{k}}^{B} = \tfrac{1}{2} \sum_{\delta} J_{\delta} B_{\delta} \cos \mathbf{k} \cdot \delta, \qquad \gamma_{\mathbf{k}}^{A} = \tfrac{1}{2} \sum_{\delta} J_{\delta} A_{\delta} \sin \mathbf{k} \cdot \delta,$$

with the sums going over all the vectors δ connecting the first and the third neighbours, N_{s} is the number of sites and real mean field parameters satisfying the relations $B_{\delta} = B_{-\delta}$ and $A_{\delta} = -A_{-\delta}$ have been assumed. The mean field Hamiltonian (7) can be diagonalized by applying a Bogoliubov transformation

$$\begin{aligned} b_{\mathbf{k}\uparrow} &= u_{\mathbf{k}} \alpha_{\mathbf{k}\uparrow} - v_{\mathbf{k}} \alpha_{-\mathbf{k}\downarrow}^{\dagger} \\ b_{\mathbf{k}\downarrow} &= u_{\mathbf{k}} \alpha_{\mathbf{k}\downarrow} + v_{\mathbf{k}} \alpha_{-\mathbf{k}\uparrow}^{\dagger}, \end{aligned} \tag{8}$$

with $u_{\mathbf{k}} = [\frac{1}{2}(1 + \frac{(\gamma_{\mathbf{k}}^{B} + \lambda)}{\omega_{\mathbf{k}}})]^{\frac{1}{2}}$ and $v_{\mathbf{k}} = \mathrm{i}\,\mathrm{sig}(\gamma_{\mathbf{k}}^{A})[\frac{1}{2}(-1 + \frac{(\gamma_{\mathbf{k}}^{B} + \lambda)}{\omega_{\mathbf{k}}})]^{\frac{1}{2}}$ the Bogoliubov coefficients, resulting in

$$\hat{H}_{\mathrm{MF}} = \sum_{\mathbf{k}} \omega_{\mathbf{k}} \left[\alpha_{\mathbf{k}\uparrow}^{\dagger} \alpha_{\mathbf{k}\uparrow} + \alpha_{-\mathbf{k}\downarrow}^{\dagger} \alpha_{-\mathbf{k}\downarrow} \right] + E_{\mathrm{MF}} \tag{9}$$

with the same free spinon dispersion relation for the up and down flavours

$$\omega_{\mathbf{k}} = \sqrt{(\gamma_{\mathbf{k}}^{B} + \lambda)^{2} - (\gamma_{\mathbf{k}}^{A})^{2}}. \tag{10}$$

The mean field free energy is given by

$$F = E_{\mathrm{MF}} + T \sum_{\mathbf{k}\sigma} \ln \left(1 - \mathrm{e}^{-\beta \omega_{\mathbf{k}\sigma}} \right), \tag{11}$$

and the self-consistent equations for the mean field parameters A_{δ}, B_{δ} and λ yield

$$A_{\delta} = \frac{1}{2N_{\mathrm{s}}} \sum_{\mathbf{k}} \frac{\gamma_{\mathbf{k}}^{\mathrm{A}}}{\omega_{\mathbf{k}}} (1 + 2n_{\mathbf{k}}) \sin \mathbf{k} \cdot \delta, \tag{12a}$$

$$B_{\delta} = \frac{1}{2N_{\mathrm{s}}} \sum_{\mathbf{k}} \frac{\gamma_{\mathbf{k}}^{\mathrm{B}} + \lambda}{\omega_{\mathbf{k}}} (1 + 2n_{\mathbf{k}}) \cos \mathbf{k} \cdot \delta, \tag{12b}$$

$$S + \frac{1}{2} = \frac{1}{2N_{\mathrm{s}}} \sum_{\mathbf{k}} \frac{\gamma_{\mathbf{k}}^{\mathrm{B}} + \lambda}{\omega_{\mathbf{k}}} (1 + 2n_{\mathbf{k}}), \tag{12c}$$

with $n_{\mathbf{k}} = (\mathrm{e}^{\beta \omega_{\mathbf{k}}} - 1)^{-1}$ the bosonic occupation number. The rotationally invariant nature of the SBMFT allows the study of magnetically disordered phases at finite temperatures in agreement with the Mermin–Wagner theorem [19]. This is manifested in the temperature dependent gapped spinon dispersion $\omega_{\mathbf{k}}$, once the self-consistent equations (12) are solved, preventing the appearance of infrared divergences in the theory. Nonetheless, as the temperature decreases the magnetic structure factor, $S(\mathbf{k}) = \sum_{\mathbf{R}} \mathrm{e}^{\mathrm{i}\mathbf{k}\cdot\mathbf{R}} \langle \hat{S}_0 \cdot \hat{S}_{\mathbf{R}} \rangle$, develops a maximum at $\mathbf{Q} = 2\mathbf{k}_{\mathrm{min}}$, with $\mathbf{k}_{\mathrm{min}}$ the minimum of the dispersion relation $\omega_{\mathbf{k}}$ [12]. For $T \to 0$, the leading order of this maximum is related to the squared magnetization and $\omega_{\mathbf{k}_{\mathrm{min}}}$ as $S(\mathbf{Q}) = \frac{1}{2N_{\mathrm{s}}} \frac{(\gamma_{\mathbf{k}_{\mathrm{min}}}^{\mathrm{B}} + \lambda)^{2}}{\omega_{\mathbf{k}_{\mathrm{min}}}^{2}} = \frac{N_{\mathrm{s}}}{2} m^{2}$. In section 2.2 it is shown how the rupture of the SU(2) symmetry is described in the zero temperature limit.

2.2. The treatment of SU(2) *broken symmetry in a spiral ground state*

The occurrence of the SU(2) broken symmetry ground state at $T = 0$ is related to the condensation of the Schwinger bosons [13, 14]. To clarify this point it is instructive to focus on the ground state wavefunction of a finite size N_{s} system. Even with semiclassical mean field solutions the ground state is magnetically disordered with a finite size gap dispersion that behaves as $\omega_{\pm\frac{\mathbf{Q}}{2}} \sim \frac{1}{N_{\mathrm{s}}}$. The positiveness of $\omega_{\mathbf{k}}$ for all $\mathbf{k}$ guarantees the diagonalization of (7), implying a zero spinon occupation number in the magnetic ground state. Using the requirement that $\alpha_{\mathbf{k}\sigma} |\mathrm{gs}\rangle = 0$, it can be easily shown that the ground state is a singlet with the following Jastrow form:

$$|\mathrm{gs}\rangle = \mathrm{e}^{\sum_{\mathbf{k}} f_{\mathbf{k}} b_{\mathbf{k}\uparrow}^{\dagger} b_{-\mathbf{k}\downarrow}^{\dagger}} |0\rangle_{b}, \tag{13}$$

where $f_{\mathbf{k}} = -v_{\mathbf{k}}/u_{\mathbf{k}}$ and $|0\rangle_{b}$ is the vacuum of Schwinger bosons b. In the thermodynamic limit $\omega_{\pm\frac{\mathbf{Q}}{2}} \to 0$ and $f_{\pm\frac{\mathbf{Q}}{2}} \to 1$, meaning that the ground state develops an infinite accumulation of spin up and down bosons at $\mathbf{k} = \pm\frac{\mathbf{Q}}{2}$. Then, the ground state can be split as

$$|\mathrm{gs}\rangle = |\phi_{\mathrm{c}}\rangle |\mathrm{gs}'\rangle,$$

where $|\phi_{\mathrm{c}}\rangle$ represents the condensed part, and

$$|\mathrm{gs}'\rangle = \mathrm{e}^{\sum_{\mathbf{k} \neq \pm\mathbf{Q}/2} f_{\mathbf{k}} b_{\mathbf{k}\uparrow}^{\dagger} b_{-\mathbf{k}\downarrow}^{\dagger}} |0\rangle_{b}$$

is the non-condensed, or normal, part of the ground state [14]. Given that the starting point (13) is a singlet, the appearance

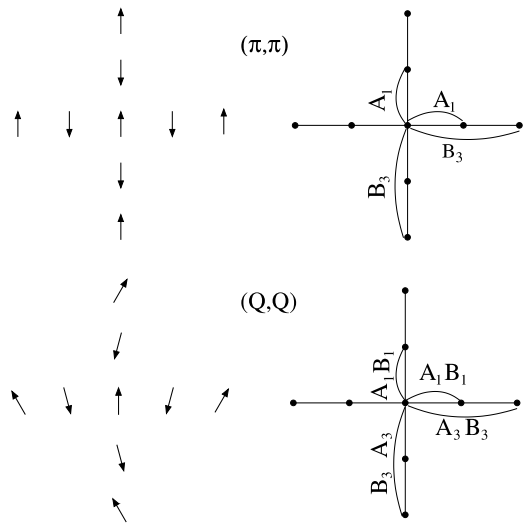

Figure 1. The mean field parameter structure corresponding to Néel (π, π) and spiral (Q, Q) correlations for the J_1–J_3 model. Only the non-vanishing parameters are indicated in each case.

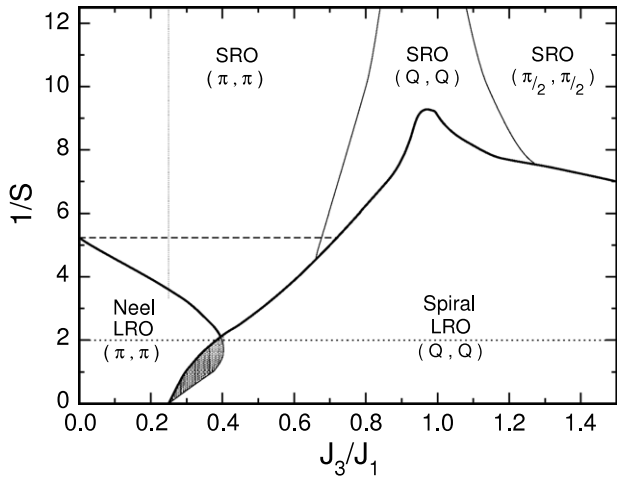

Figure 2. The magnetic phase diagram for the J_1–J_3 model predicted by the SBMF. Solid lines represent continuous or second order transitions. Thin lines denote disorder lines between different SRO regimes. The hatched area is a metastable Néel region and the dotted line indicates the $S = 1/2$ case. The dashed horizontal line corresponds to the SBMF prediction within the one singlet decoupling for the Néel phase (see text).

of the condensate must be related to the rupture of the SU(2) symmetry. Physically, this can be thought of by considering the hypothetical process of switching on a modulated magnetic field h with pitch $\mathbf{Q}$, then taking the thermodynamic limit $N_s \to \infty$, and finally taking the limit $h \to 0$ [13, 12]. For instance, a coherent state

$$|\phi_c\rangle = e^{\sqrt{\frac{N_s m}{2}}\left(b^\dagger_{\frac{\mathbf{Q}}{2}\uparrow} + b^\dagger_{-\frac{\mathbf{Q}}{2}\uparrow} + ib^\dagger_{\frac{\mathbf{Q}}{2}\downarrow} - ib^\dagger_{-\frac{\mathbf{Q}}{2}\downarrow}\right)}|0\rangle_b \qquad (14)$$

thus selected gives a quantum spiral state with magnetization m and spiral pitch $\mathbf{Q}$ lying in the x–z plane. In fact, the mean value of the spin operator in this state yields

$$\langle gs|\hat{S}^x_i|gs\rangle = m\sin(\mathbf{Q}\cdot\mathbf{r}_i); \qquad \langle gs|\hat{S}^y_i|gs\rangle = 0;$$
$$\langle gs|\hat{S}^z_i|gs\rangle = m\cos(\mathbf{Q}\cdot\mathbf{r}_i);$$

while the local magnetization m and the condensate of bosons are related by

$$\langle\phi_c|b_{\mathbf{k}\uparrow}|\phi_c\rangle = \left(\frac{N_s m}{2}\right)^{\frac{1}{2}}(\delta_{\mathbf{k},\frac{\mathbf{Q}}{2}} + \delta_{\mathbf{k},-\frac{\mathbf{Q}}{2}})$$
$$\langle\phi_c|b_{\mathbf{k}\downarrow}|\phi_c\rangle = i\left(\frac{N_s m}{2}\right)^{\frac{1}{2}}(\delta_{\mathbf{k},-\frac{\mathbf{Q}}{2}} - \delta_{\mathbf{k},\frac{\mathbf{Q}}{2}}), \qquad (15)$$

which in real space implies a mean value of the spinors of the form

$$\begin{pmatrix}\langle\phi_c|b_{i\uparrow}|\phi_c\rangle\\ \langle\phi_c|b_{i\downarrow}|\phi_c\rangle\end{pmatrix} = \sqrt{2m}\begin{pmatrix}\cos\dfrac{\mathbf{Q}\cdot\mathbf{r}_i}{2}\\ \sin\dfrac{\mathbf{Q}\cdot\mathbf{r}_i}{2}\end{pmatrix}.$$

Replacing these values in (5) one obtains the semiclassical expressions for the mean field parameters

$$A_\delta = \langle\phi_c|\hat{A}^\dagger_\delta|\phi_c\rangle = m\sin\frac{\mathbf{Q}\cdot\delta}{2},$$
$$B_\delta = \langle\phi_c|\hat{B}^\dagger_\delta|\phi_c\rangle = m\cos\frac{\mathbf{Q}\cdot\delta}{2} \qquad (16)$$

which are consistent with the real nature of the mean field parameters assumed above. This procedure can be performed for a quantum spiral state with magnetization lying in the y–z plane. In this case the same semiclassical forms (16) are recovered but with $\langle\phi_c|\hat{A}^\dagger_\delta|\phi_c\rangle$ imaginary pure. It is interesting to note that both mean field solutions are related by a global gauge transformation $b_{i\sigma} \to e^{i\theta}b_{i\sigma}$ with $\theta = -\pi/4$. On the other hand, complex values of the mean field parameters A_δ and B_δ can be related to the existence of non-coplanar magnetic or chiral spin liquid states which will be not studied in this work. For a detailed study of the complex solutions see [6].

Using (16), the semiclassical magnetic structures are related to the mean field parameters in the following way (see figure 1): (a) for Néel $\mathbf{Q} = (\pi, \pi)$ order, $A_{1x} = A_{1y} = A_1 \neq 0$ and $B_{1x} = B_{1y} = B_1 = 0$, while $A_{3x} = A_{3y} = A_3 = 0$ and $B_{3x} = B_{3y} = B_3 \neq 0$; (b) for spiral $\mathbf{Q} = (Q, Q)$ order, $A_{1x} = A_{1y} = A_1 \neq 0$, $B_{1x} = B_{1y} = B_1 \neq 0$, $A_{3x} = A_{3y} = A_3 \neq 0$ and $B_{3x} = B_{3y} = B_3 \neq 0$. We have found that this parameter structure is the same for the LRO and SRO cases, regardless of the quantum or thermal nature of the fluctuations. It is worth stressing that for a Néel phase frustration J_3 is taken into account through the parameter B_3, whereas for the one operator scheme of decoupling there is no mean field parameter sensitive to frustration since $A_3 = 0$ (its physical consequence is clearly reflected in the local magnetization, see figure 3).

To study SU(2) broken symmetry states, the self-consistent equations (12) must be re-calculated taking into account explicitly the condensate (14) in the thermodynamic limit. The new set of self-consistent equations results as

$$A_\delta = m\sin\frac{\mathbf{Q}\cdot\delta}{2} + \int_{\mathbf{k}}\frac{\gamma^A_{\mathbf{k}}}{\omega_{\mathbf{k}}}\sin\mathbf{k}\cdot\delta\ d\mathbf{k} \qquad (17a)$$

$$B_\delta = m\cos\frac{\mathbf{Q}\cdot\delta}{2} + \int_{\mathbf{k}} \frac{\gamma^B_{\mathbf{k}} + \lambda}{\omega_{\mathbf{k}}} \cos\mathbf{k}\cdot\delta \; \mathrm{d}\mathbf{k} \quad (17b)$$

$$S + \frac{1}{2} = m + \int_{\mathbf{k}} \frac{\gamma^B_{\mathbf{k}} + \lambda}{\omega_{\mathbf{k}}} \; \mathrm{d}\mathbf{k}. \quad (17c)$$

In addition to the parameters A_δ, B_δ, and λ, the magnetization m enters as a new self-consistent parameter. From a comparison with (12) it follows that the condensate components of (17) correspond to the separate treatment of the singular modes $\mathbf{k} = \pm\frac{\mathbf{Q}}{2}$ of the dispersion relation $\omega_{\mathbf{k}}$ whereas the sums of (12) are transformed into integrals, as usually presented in the literature [13]. On the other hand, the magnon excitations of the quantum spiral state are obtained by computing the dynamical magnetic structure factor [11, 12]. Here, the spectrum of the $S^\dagger_{\mathbf{k}}$ excitations is composed of a pair-spinon continuum with the lowest energy process consisting of destroying one Schwinger boson $b_{\pm\frac{\mathbf{Q}}{2}\downarrow}$ from the condensate and creating another one $b^\dagger_{\mathbf{k}\pm\frac{\mathbf{Q}}{2}\uparrow}$ in the normal fluid part [32]. Given that $\omega_{\pm\frac{\mathbf{Q}}{2}} = 0$, the energy cost of such a spin-1 excitation with momentum $\mathbf{k}$ is $\omega_{\mathbf{k}\pm\frac{\mathbf{Q}}{2}}$.

The dispersion relation of the spin-1 excitation in the large S limit results as

$$\omega_{\mathbf{k}\pm\frac{\mathbf{Q}}{2}} = S\sqrt{[J_{\mathbf{k}} - J_{\mathbf{Q}}][J_{\mathbf{k}\pm\mathbf{Q}} - J_{\mathbf{Q}}]}, \quad (18)$$

where (16) has been replaced in the shifted spinon dispersion $\omega_{\mathbf{k}\pm\frac{\mathbf{Q}}{2}}$, $\lambda = -SJ_{\mathbf{Q}}$ and $J_{\mathbf{k}} = \sum_\delta J_\delta \mathrm{e}^{\mathrm{i}\mathbf{k}\cdot\delta}$. The two possible dispersion relations, $\omega_{\mathbf{k}+\frac{\mathbf{Q}}{2}}$ and $\omega_{\mathbf{k}-\frac{\mathbf{Q}}{2}}$, do not coincide with the semiclassical linear spin wave (LSW) expression

$$\omega^{\mathrm{LSW}}_{\mathbf{k}} = S\sqrt{[J_{\mathbf{k}} - J_{\mathbf{Q}}][(J_{\mathbf{k}+\mathbf{Q}} + J_{\mathbf{k}+\mathbf{Q}})/2 - J_{\mathbf{Q}}]}. \quad (19)$$

In fact, to recover the conventional spin wave result singlet and triplet mean field parameters must be introduced [14]. Nonetheless both (18) and (19) have the same zero energy *star* modes $\mathbf{k} = (0,0), (\pm Q, \pm Q), (\pm Q, \mp Q)$ [14]. For a given spiral order (Q, Q) one expects only three zero Goldstone modes related to the complete rupture of the $SO(3)$ symmetry, whereas the spurious zero modes $(\pm Q, \mp Q)$ reflect the lattice symmetry in the spectrum. For example, the spiral (Q, Q) is related to the spirals $(Q, -Q)$ and $(-Q, Q)$ by a global rotation combined with a reflexion about y and x, respectively [24]. In the quantum $S = \frac{1}{2}$ case, however, after the iterative procedure, the SBMF dispersion recovers the correct Goldstone mode structure at $\mathbf{k} = (0,0), (\pm Q, \pm Q)$ for spiral antiferromagnets, whereas in the spin wave theory the removal of the spurious zero modes requires one to go beyond the harmonic approximation [34]. Regarding the functional form of the physical dispersion one could take the minimum of $\{\omega_{\mathbf{k}+\frac{\mathbf{Q}}{2}}, \omega_{\mathbf{k}-\frac{\mathbf{Q}}{2}}\}$ as the lowest energy excitation for each $\mathbf{k}$. Nonetheless, we have recently shown that for the 120° Néel order of a spin-$\frac{1}{2}$ triangular antiferromagnet it is possible to recover the correct dispersion relation—found with series expansions [35] and LSW plus $\frac{1}{S}$ corrections [36]—by a proper reconstruction based on the shifted spinon dispersion parts of $\omega_{\mathbf{k}\pm\frac{\mathbf{Q}}{2}}$ that concentrate the greater spectral weight of the dynamical structure factor [32]. It is worth stressing that at the mean field level the two spinons building up the magnon-like excitation are free but, after corrections to the SBMF, one expects low energy tightly bound pairs of spinons merging from the continuum [33].

3. Results

3.1. Zero temperature quantum phase diagram

To obtain the zero temperature quantum phase diagram of the J_1–J_3 model for arbitrary S we have computed numerically the self-consistent equations (17) as follows. Using (16), a classical structure—A^0_δ, B^0_δ. $m^0 = S$, and $\mathbf{Q}^0$—is replaced in the spinon dispersion relation (10), in order to get the value of λ^0 that makes the spinon dispersion gapless, $(\gamma^{B^0}_{\pm\mathbf{Q}^0/2} + \lambda^0)^2 = |\gamma^{A^0}_{\pm\mathbf{Q}^0/2}|^2$. From (17*c*) one obtains m^0 and then A^0_δ, B^0_δ, $\mathbf{Q}^0$, λ^0 and m^0 are plugged into (17*a*) and (17*b*) to obtain the new parameters A^1_δ, B^1_δ. Noting that the new minimum $\mathbf{k}_{\min}$ of $\omega_{\mathbf{k}}$ is related to the new spiral pitch as $\mathbf{Q}^{(1)} = 2\mathbf{k}_{\min}$, the iteration is continued until the process converges. Depending on the quantum fluctuation strength, which can be measured by the value of S, there are solutions with Néel and spiral correlations but with $m = 0$. We have called these solutions short range order (SRO) (π, π) and SRO (Q, Q), respectively.

Figure 2 shows the phase diagram predicted by the SBMF for all spin and several frustration values.

Long range order regimes. For $S = \infty$ one recovers the classical continuous transitions at $J_3/J_1 = 0.25$ between LRO Néel and LRO spiral phases [22]. As S is decreased there is an enhancement of the stability of the Néel phase accompanied by a similar reduction of the stability of the spiral phase. This behaviour was predicted some time ago using symmetry arguments [23]. At the transition line of this regime (solid line) the magnetic wavevector changes continuously from (π, π) to incommensurate spiral orders as the frustration is increased. For spin values $S \gtrsim \frac{1}{2}$ there is a metastable Néel region characterized by a reentrance shown in the hatched area of figure 2. This behaviour is characteristic of the non-trivial interplay between frustration and quantum fluctuations taken into account by the two singlet operator scheme. In particular, it has already been found with the same approximation in related models like the J_1–J_2 or $J_2 = 2J_3$ line of the J_1–J_2–J_3 model on the square [20, 37, 29] and the honeycomb [38, 39] lattice. If the one singlet operator scheme is applied the solid line delimiting the LRO Néel phase should be replaced by the dashed horizontal line of figure 2, missing completely the effect of frustration for the Néel phase [15, 41]. The reason for this artefact has already been discussed in section 2.2. For spin values $S \lesssim 0.5$, the continuous transition turns out to be a second order transition between LRO and SRO states.

Short range order regimes. The study of the phase diagram for the non-physical case $S < \frac{1}{2}$ is interesting as one can get an insight into the possible quantum effects beyond the mean field approximation for the physical case $(S = \frac{1}{2})$. In these regimes successive SRO transitions take place across the disorder lines [40] (thin lines), $(\pi, \pi) \leftrightarrow (Q, Q) \leftrightarrow (\frac{\pi}{2}, \frac{\pi}{2})$,

as the frustration is varied. Here, the mean field solutions can be related to the large N limit solutions, $\kappa = \frac{2S}{N}$, where spinons are exactly free only for $\kappa = 0$. Inclusion of finite N fluctuations may change the nature of the ground state and the excitations drastically. In this sense, effective gauge field theories predict that a commensurate SRO ground state is unstable towards a valence bond solid order with confined spinons while in the incommensurate SRO case a Z_2 spin liquid state with deconfined spinons is stabilized [15]. This physical picture, of course, is beyond the scope of the mean field approximation whose main weakness resides in the relaxation of the local constraint. For the regime $S \to 0$ we have found that the two thin lines, separating SRO (π, π) and $(\frac{\pi}{2}, \frac{\pi}{2})$ states, converge into one line (not shown in figure 2) at about $J_3/J_1 \sim 1$. For $J_3/J_1 < 1$ ($J_3/J_1 > 1$) only $A_{1x} = A_{1y} = A_1 \neq 0$ ($A_{3x} = A_{3y} = A_3 \neq 0$) survives, respectively. These states that only form singlet bonds A_δ along the links of largest J_δ coincide with a family of solutions coined *greedy bosons*, found within the context of the large N theory for $\kappa \to 0$ [42]. Furthermore, this kind of solution is in agreement with the upper bounds for the mean field parameters, $|A_{ij}| \leq 2S + \frac{1}{2}$ and $|B_{ij}| \leq S$, recently pointed out in [6]. On the other hand, one can notice the ample room for stability of the SRO (π, π) phase. In fact, the extended line transition between LRO spirals and SRO Néel (π, π) phases, about $0.4 \lesssim J_3/J_1 \lesssim 0.65$, implies a tendency of quantum fluctuations to form commensurate magnetic correlations which in turn will favour valence bond solid states [15]. Based on our previous work [30], we can safely estimate that Gaussian fluctuations will increase the stability of the SRO (π, π) and SRO (Q, Q), pushing the LRO (π, π) and (Q, Q) phases towards higher values of S, and thus opening an intermediate disordered window with probably a valence bond solid or Z_2 spin liquid character.

Spin $S = \frac{1}{2}$ case. These results are particularly interesting due to the further comparison with the available numerical studies. In figure 3 the local magnetization versus the frustration is plotted for $S = \frac{1}{2}$. There is a continuous transition from Néel to spiral phases that turns out to be quasi-critical at $(J_3/J_1)_c \sim 0.38$ with quite a small local magnetization $m \sim 0.015$. In the same figure 3 the dashed line shows the prediction of the one singlet operator $\hat{A}_{ij}$ scheme. Although the transition occurs at the same point, the approximation fails to describe the frustration effects for the Néel phase as discussed above for the $\frac{1}{S}$ phase diagram (figure 2). The inset of figure 3 shows the continuous variation of the magnetic wavevector $\mathbf{Q}$ with frustration (solid line) where a strong quantum renormalization with respect to the classical value [22] (dotted line) is observed. For spiral phases, both schemes of decoupling, one and two singlet operators, predict the same value of $\mathbf{Q}$ (solid line). Regarding the numerical studies for $S = \frac{1}{2}$, they predict the existence of an intermediate disordered regime in the range $0.4 \lesssim J_3/J_1 \lesssim 0.8$ with, probably, SRO plaquette and SRO spiral regimes between LRO Néel and LRO spiral phases [25–27], while for the special case $J_3/J_1 \simeq 0.5$ there is evidence of a homogeneous spin liquid state [28]. From our previous work [30], we again estimate that corrections to the mean field will open

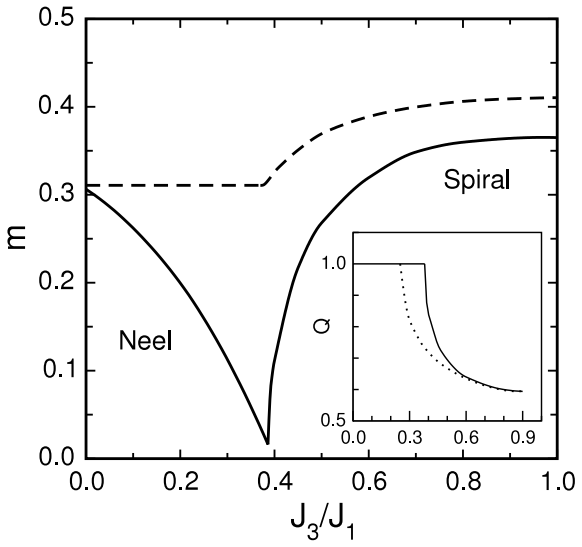

Figure 3. The local magnetization m as a function of the frustration for the case $S = \frac{1}{2}$. The solid line is for the two singlet operator scheme and the dashed line is for the one singlet operator scheme. In both schemes the transition point occurs at the value $(J_3/J_1)_c \sim 0.38$. Inset: the Q value, in units of π, of the magnetic wavevector (Q, Q) versus the frustration.

a disordered window with SRO (π, π) correlations around the critical value $(J_3/J_1)_c \sim 0.38$. By noting that the mean field on site spin fluctuations $\langle \hat{\mathbf{S}}_i^2 \rangle = \frac{3}{8} 2S(2S + 2)$ do not coincide with the expected value $S(S + 1)$, one can choose S in order to adjust the correct local spin fluctuations [6]. This procedure gives a spin value $S^* = \frac{1}{2}(\sqrt{3} - 1) \sim 0.366$ that, from inspection of figure 2 at $\frac{1}{S^*} \sim 2.73$, implies an SRO Néel region within the range $0.35 \lesssim J_3/J_1 \lesssim 0.5$. Since these states have a tendency to form valence bond solid states [15] we conclude that reasonable agreement with numerical results [27] will be found. However, to recover the homogeneous spin liquid state found at $J_3/J_1 = 0.5$ one should improve the calculation, for example, implementing the local constraint exactly. Recent variational Monte Carlo studies based on the SBMF ansatz [9] predict a Z_2 spin liquid state in the disordered regime of the J_1–J_2 model, even in the absence of spiral SRO [15]. Therefore, in agreement with [28], we also expect the probable realization of a Z_2 spin liquid in the disordered region of the J_1–J_3 model. Recently, similar features have been found using the same approximation for the phase diagram of the J_1–J_2 model on the honeycomb lattice [43].

3.2. Finite temperature phase diagram

The finite temperature phase diagram is obtained by solving the self-consistent equations (12) with the mean field parameters A_δ, B_δ, and λ. Here, in agreement with the Mermin–Wagner theorem, the magnetization m always gives zero. This rotationally invariant solution corresponds to the renormalized classical regime with an exponential decay of the spin–spin correlation functions [44]. In particular, we are mainly interested in the SRO spiral phases since at finite

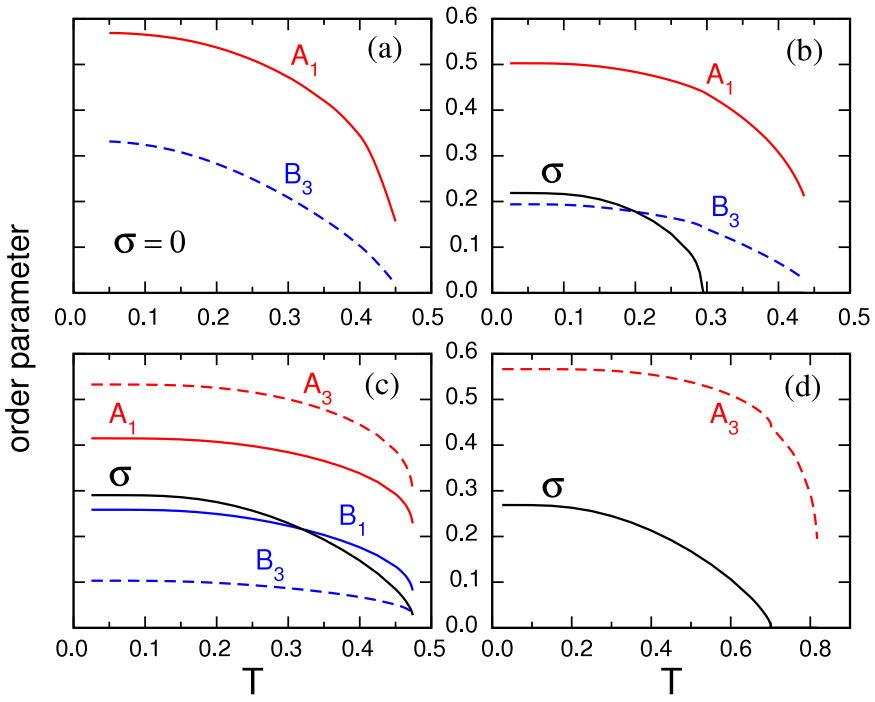

Figure 4. The mean field and nematic order parameters versus the temperature for several frustration values. (a) $J_3/J_1 = 0.3$, (b) $J_3/J_1 = 0.6$, (c) $J_3/J_1 = 1$ and (d) $J_3/J_1 = 1.8$.

temperature they break the discrete Z_2 symmetry relating the (Q, Q) and $(Q, -Q)$ phases. In fact, classical Monte Carlo results [24] predict a Z_2 broken symmetry phase that belongs to the Ising universality class characterized by the *nematic* order parameter

$$\sigma = \langle \hat{\mathbf{S}}_1 \cdot \hat{\mathbf{S}}_3 - \hat{\mathbf{S}}_2 \cdot \hat{\mathbf{S}}_4 \rangle, \tag{20}$$

where the numbers denote the sites of a single square plaquette ordered in the cyclic form $(1, 2, 3, 4)$ [24]. Besides giving a measure of spiral correlations—it vanishes for Néel correlations—it is easy to see that the order parameter σ assumes opposite signs for (Q, Q) and $(Q, -Q)$ correlations. To compute σ within the SBMF theory it is sufficient to resort to (4), whence σ is written in terms of second neighbour correlations as

$$\sigma = B_{13}^2 - A_{13}^2 - B_{24}^2 + A_{24}^2. \tag{21}$$

Although the mean field parameters are the As and Bs to first and third neighbours, it is possible to calculate B_{13}, B_{24}, A_{13} and A_{24} by solving first the self-consistent equation (12) and then computing (12*a*) and (12*b*) with the vector δ connecting second neighbours $(1, 1)$ and $(1, -1)$. On the other hand, by plugging in the semiclassical expressions (16) the order parameter results as

$$\sigma = -2S^2 \sin Q_x \cdot \sin Q_y,$$

where the sign difference between (Q, Q) and $(Q, -Q)$ states is evident, as expected.

Depending on the frustration value we have found different regimes as the temperature is increased from the zero temperature ground states. Figure 4(a) shows the temperature dependence of the non-zero parameters A_1 and B_3 corresponding to a Néel phase at $J_3/J_1 = 0.3$. The parameters decrease monotonically, giving rise to an SRO Néel phase until $T \sim 0.45$. Beyond this temperature the SBMF gives a perfect paramagnet with all the mean field parameters equal to zero. Starting from a spiral ground state, two different temperature behaviours are observed. On one hand, for $0.38 < J_3/J_1 < 1$, the phase with SRO spiral phase undergoes a transition to SRO Néel phase as the temperature increases, since fluctuations above a collinear SRO can minimize the free energy more efficiently. This behaviour, already observed in related models [45], is shown in figure 4(b) for $J_3/J_1 = 0.6$. Here, the spiral correlations signalled by $\sigma \neq 0$ persist until $T \sim 0.3$, while for higher temperatures SRO Néel correlations are stabilized—$A_1, B_3 \neq 0$—until the value $T \sim 0.45$ is reached. On the other hand, for $J_3/J_1 > 1$, before reaching the paramagnetic phase there is again an intermediate collinear phase that we have named $(\pi, \pi)_4$ because it is composed of four decoupled third neighbour sublattices with SRO Néel correlations in each one (see figure 5). In this way the free energy can be more efficiently minimized since thermal fluctuations above such a decoupled collinear AF SRO between third neighbours optimize both the internal energy and the entropy. This is shown in figure 4(d) for $J_3/J_1 = 1.8$ where only the AF mean field parameter A_3 survives along with a weaker ferromagnetic correlation between fifth neighbours B_5 (not shown in the figure), and so forth, within the range $0.7 < T < 0.8$. Figure 4(c) shows the special case $J_3/J_1 = 1$ where there is a direct transition from an SRO spiral phase to a perfect paramagnet at around $T = 0.45$.

The jumps of A_1 and A_3 found at this temperature (figure 4) are due to the difficulty in solving numerically

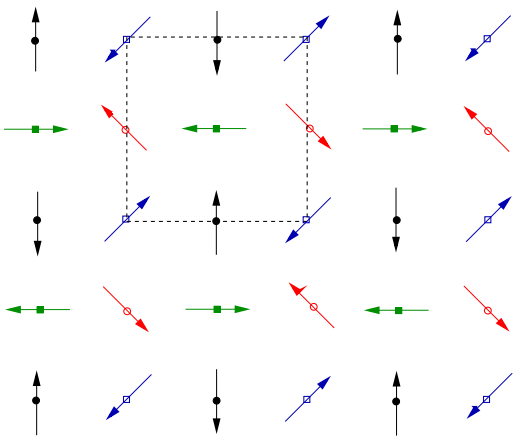

Figure 5. Schematic magnetic structure corresponding to the $(\pi,\pi)_4$ phase composed of four decoupled third neighbour sublattices with Néel correlations in each one.

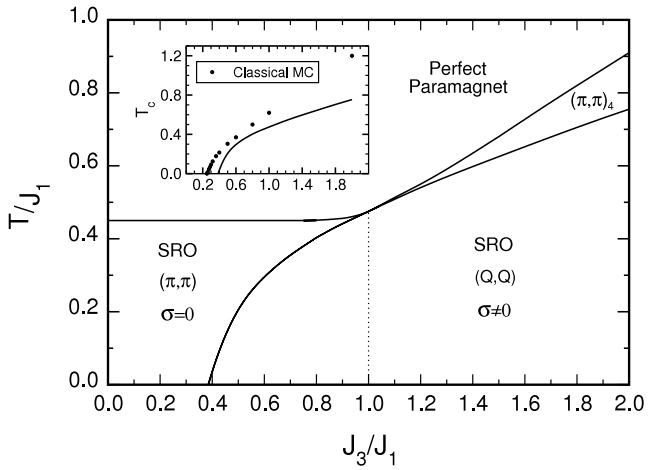

Figure 6. The finite temperature phase diagram for the $S = \frac{1}{2}$ case of the J_1–J_3 model. Inset: the critical temperature T_c for the Z_2 broken symmetry phase versus the frustration predicted by classical Monte Carlo [24] (dots) and SBMF (solid line).

the constraint equation around $T = 0.45$. Actually, on approaching from high temperatures, it can be shown analytically that in certain limits A_1 and A_3 go continuously to zero [20]. In this regime all mean field parameters are zero and the constraint (12*c*) implies

$$\omega_{\mathbf{k}} = \lambda = T \ln\left(1 + \frac{1}{S}\right). \tag{22}$$

Then, assuming that in the limit $J_1 \gg J_3$ the first mean field parameter that switches on is A_1 with its semiclassical form, equation (12*a*) yields

$$\frac{1}{J_1} = \frac{1}{2N} \sum_{\mathbf{k}} \frac{(\sin^2 k_x + \sin k_y \sin k_x)}{\omega_{\mathbf{k}}} (1 + 2n_{\mathbf{k}}). \tag{23}$$

Replacing (22) and carrying on the two-dimensional integral of (23) one obtains the critical temperature

$$T_1^* = \frac{J_1}{2} \frac{(\frac{1}{2} + S)}{\ln(1 + \frac{1}{S})}.$$

For $S = \frac{1}{2}$ this temperature, $T_1^* \simeq 0.45$, coincides with the horizontal boundary between the paramagnetic phase and the SRO Néel phase ($J_3/J_1 < 1$) of the finite temperature phase diagram (figure 6) found numerically. A similar procedure can be carried out for A_3 in the limit $J_3 \gg J_1$, giving the critical temperature

$$T_3^* \sim \frac{J_3}{2} \frac{(\frac{1}{2} + S)}{\ln(1 + \frac{1}{S})}.$$

Again, for $S = \frac{1}{2}$, this gives a linear behaviour $T_3^* \sim 0.45 J_3$ that agrees with the boundary between the paramagnetic regime and the $(\pi,\pi)_4$ regime of the finite temperature phase diagram (figure 6). On the other hand, the boundary of the Z_2 broken symmetry regime has been numerically identified with the temperature T_c where the nematic order parameter σ goes to zero. The inset of figure 6 shows the qualitative good agreement for the critical temperature T_c of the Z_2 broken symmetry phase, as a function of the frustration, predicted by classical Monte Carlo and SBMF theory. Given that the SBMF recovers the classical result in the large S limit, the slight shift to the right of T_c with respect to classical MC results can be interpreted as the quantum effect for the $S = \frac{1}{2}$ case. Actually, we expect an even more marked shift once corrections above the SBMF are computed.

4. Concluding remarks

We have investigated the rupture of the discrete and continuous symmetries in the frustrated J_1–J_3 Heisenberg model using Schwinger boson mean field theory. We have studied in detail both the SU(2) broken symmetry which has been explicitly related to the condensate part of the ground state wavefunction and the Z_2 broken symmetry related to the rupture of the discrete degeneracy of the (Q, Q) and $(Q, -Q)$ phases. By comparing with already existent results, we have shown that the two singlet bond operator scheme of the SBMF gives reliable results for the zero temperature quantum phase diagram. In particular, this scheme describes correctly the expected effects of frustration in the collinear phase [23] that are not captured by the one singlet scheme used in the literature [15]. For $S = \frac{1}{2}$, local spin fluctuation considerations allow us to infer a disordered regime $0.35 \lesssim J_3/J_1 \lesssim 0.5$ that qualitatively agrees with recent numerical results [27]. Regarding the finite temperature regime, we have found a Z_2 broken symmetry phase characterized by the nematic order parameter σ with the rotational invariance restored. The behaviour of the critical temperature T_c versus the frustration agrees qualitatively well with classical Monte Carlo results [24]. Based on these classical MC results, the possible realization of a Z_2 spin liquid with nematic order in the limit $T \to 0$ between the Néel and spiral phases has been suggested [24]. It should be noticed, however, that in principle there is no connection between the Z_2 global symmetry of the Ising-like nematic order parameter σ and the Z_2 gauge theory of the spin liquid phase. In the context of the low energy effective field theory the Z_2 gauge symmetry corresponds to the Z_2 gauge invariance of

some spinor fields, analogous to the Schwinger boson spinors, that results from a particular parametrization of the spiral order [7, 46]. In the present microscopic SBMF the studied quantum and finite temperature solutions are of the same nature, with a finite Ising-like nematic order; consequently, it is important to remark that, if the Z_2 spin liquid exists, its non-trivial properties will appear, for instance, by solving the hard core local constraint exactly. Nonetheless, at present, its implementation within the variational Monte Carlo shows severe limitations allowing the study of system sizes up to 6×6 [9, 10, 47]. Another interesting result is the general tendency of thermal fluctuations to stabilize collinear correlations. In particular, we have found transitions from spiral SRO to collinear Néel SRO before reaching the paramagnetic phase: for $J_3/J_1 < 1$ short range Néel (π, π) correlations are favoured while for $J_3/J_1 > 1$ there is an intermediate phase $(\pi, \pi)_4$ characterized by four decoupled third neighbour sublattices with SRO Néel correlations in each one. Classical Monte Carlo is required for the study of the $(\pi, \pi)_4$ phase.

We have shown that the Schwinger boson mean field theory is a simple and versatile tool that, once adequately implemented, is able to recover the main features of frustrated Heisenberg models such as static, dynamic and finite temperature properties. It would be interesting to extend the study to doped frustrated antiferromagnets within the context of the $t - J$ model [48], where it is known that spiral fluctuations change the hole spectral functions drastically [49]. Furthermore, the two singlet bond operator scheme used in this work can be properly extended to the study of anisotropic frustrated models. In particular, for the XXZ model on the triangular lattice we have found [50] that the SBMF recovers the dispersion relation predicted by the spin wave plus $1/S$ corrections [36].

Acknowledgments

We thank L Capriotti for sending us his Monte Carlo results. This work was supported by CONICET under grant PIP2009 No 1948.

References

[1] Anderson P W 1987 *Science* **235** 1196
[2] Misguich G and Lhuillier C 2005 Two-dimensional quantum antiferromagnets *Frustrated Spin Systems* ed H T Diep (Singapore: World Scientific) chapter 5, pp 229–306
[3] Balents L 2010 *Nature* **464** 199
[4] Wen X G 2002 *Phys. Rev.* B **65** 165113
[5] Wang F and Vishwanath A 2006 *Phys. Rev.* B **74** 174423
[6] Messio L, Lhuillier C and Misguich G 2013 *Phys. Rev.* B **87** 125127
[7] Powell B J and McKenzie R H 2011 *Rep. Prog. Phys.* **74** 056501
[8] Jiang H C, Yao H and Balents L 2012 *Phys. Rev.* B **86** 024424
[9] Li T, Becca F, Hu W and Sorella S 2012 *Phys. Rev.* B **86** 075111
[10] Hu W J, Becca F, Parola A and Sorella S 2013 *Phys. Rev.* B **88** 060402
[11] Arovas D P and Auerbach A 1988 *Phys. Rev.* B **38** 316
Auerbach A and Arovas D P 1988 *Phys. Rev. Lett.* **61** 617
[12] Auerbach A 1994 *Interacting Electrons and Quantum Magnetism* (Berlin: Springer)
[13] Sarker S, Jayaprakash C, Krishnamurthy H R and Ma M 1989 *Phys. Rev.* B **40** 5028
[14] Chandra P, Coleman P and Larkin A I 1990 *J. Phys.: Condens. Matter* **2** 7933
[15] Read N and Sachdev S 1991 *Phys. Rev. Lett.* **66** 1773
Sachdev S and Read N 1991 *Int. J. Mod. Phys.* B **5** 219
[16] Chandra P and Doucot B 1988 *Phys. Rev.* B **38** 9335
[17] Richter J and Schulenburg J 2010 *Eur. Phys. J.* B **73** 117 (and references therein)
[18] Chandra P, Coleman P and Larkin A I 1990 *Phys. Rev. Lett.* **64** 88
[19] Mermin N D and Wagner H 1966 *Phys. Rev. Lett.* **17** 1133
[20] Flint R and Coleman P 2008 *Phys. Rev.* B **79** 014424
[21] Weber C, Capriotti L, Misguich G, Becca F, Elhajal M and Mila F 2003 *Phys. Rev. Lett.* **91** 177202
Capriotti L, Fubini A, Roscilde T and Tognetti V 2004 *Phys. Rev. Lett.* **92** 157202
[22] Locher P 1990 *Phys. Rev.* B **41** 2537
[23] Ferrer J 1993 *Phys. Rev.* B **47** 8769
[24] Capriotti L and Sachdev S 2004 *Phys. Rev. Lett.* **93** 257206
[25] Leung P W and Lam N W 1996 *Phys. Rev.* B **53** 2213
[26] Mambrini M, Läuchli A, Poilblanc D and Mila F 2006 *Phys. Rev.* B **74** 144422
[27] Reuther J, Wölfle P, Darradi R, Brenig W, Arlego M and Richter J 2011 *Phys. Rev.* B **83** 064416
[28] Capriotti L, Scalapino D J and White S R 2004 *Phys. Rev. Lett.* **93** 177004
[29] Ceccatto H A, Gazza C J and Trumper A E 1993 *Phys. Rev.* B **47** 12329
[30] Trumper A E, Manuel L O, Gazza C J and Ceccatto H A 1997 *Phys. Rev. Lett.* **78** 2216
[31] Manuel L O, Trumper A E and Ceccatto H A 1998 *Phys. Rev.* B **57** 8348
[32] Mezio A, Sposetti C N, Manuel L O and Trumper A E 2011 *Europhys. Lett.* **94** 47001
[33] Mezio A, Manuel L O, Singh R R P and Trumper A E 2012 *New J. Phys.* **14** 123033
[34] Rastelli E and Tassi A 1992 *J. Phys.: Condens. Matter* **4** 1567
[35] Zheng W, Fjaerestad J O, Singh R R P, McKenzie R H and Coldea R 2006 *Phys. Rev.* B **74** 224420
[36] Chernyshev A L and Zhitomirsky M E 2009 *Phys. Rev.* B **79** 144416
[37] Mila F, Poilblanc D and Bruder C 1991 *Phys. Rev.* B **43** 7891
[38] Mattsson A, Fröjdh P and Einarsson T 1994 *Phys. Rev.* B **49** 3997
[39] Cabra D C, Lamas C A and Rosales H D 2011 *Phys. Rev.* B **83** 094506
[40] Selke W 1992 Spatially modulated structures in systems with competing interactions *Phase Transitions and Critical Phenomena* vol 15, ed C Domb and J L Lebowitz (New York: Academic) chapter 1, pp 1–72
[41] Chung C H, Marston J B and McKenzie R H 2001 *J. Phys.: Condens. Matter* **13** 5159
[42] Tchernyshyov O, Moessner R and Sondhi S L 2006 *Europhys. Lett.* **73** 278
[43] Zhang H and Lamas C A 2013 *Phys. Rev.* B **87** 024415
[44] Yoshioka D and Miyazaki J 1991 *J. Phys. Soc. Japan* **60** 614
[45] Hauke P, Roscilde T, Murg V, Cirac J I and Schmied R 2010 *New J. Phys.* **12** 053036
[46] Sachdev S 2008 *Nature Phys.* **4** 173
[47] Tay T and Motrunich O I 2011 *Phys. Rev.* B **84** 020404
[48] Kane C L, Lee P A and Read N 1989 *Phys. Rev.* B **39** 6880
[49] Trumper A E, Gazza C J and Manuel L O 2004 *Phys. Rev.* B **69** 184407
Trumper A E, Gazza C J and Manuel L O 2004 *Physica* B **354** 252
Hamad I J, Manuel L O and Trumper A E 2012 *Phys. Rev.* B **85** 024402
[50] Ghioldi E A, Mezio A, Manuel L O and Trumper A E 2013 in preparation